Available online at www.sciencedirect.com

ScienceDirect

Physics Procedia 47 (2013) 131 – 136

Physics Procedia

Scientific Workshop on Nuclear Fission Dynamics and the Emission of Prompt Neutrons and Gamma Rays, Biarritz, France, 28-30 November 2012

Corrections of prompt-neutron emission in fission-fragment experiments

A. Al-Adili[a,b,*], F.-J. Hambsch[a], S. Pomp[b], S. Oberstedt[a]

[a] *European Commission - DG Joint Research Centre (IRMM), B-2440 Geel, Belgium*
[b] *Division of Applied Nuclear Physics, Uppsala University, S-751 20 Uppsala, Sweden*

Abstract

The number of emitted prompt neutrons in the fission process is strongly dependent on the fragment mass. The deformation of the fragments as well as shell effects give the characteristic "sawtooth" shape. It is well known that the total average neutron emission ($\bar{\nu}_{\rm tot}$) increases as a function of incident-neutron energy. But do these extra emitted neutrons also show a particular dependence on the fragment mass? Some experiments have shown that the additional neutrons are emitted from the heavy fragments only. Recent theoretical studies provided an explanation for this, thus emphasising the validity of these observations. Despite this, in various experiments and calculations an average increase of $\bar{\nu}(A)$ was and is still assumed. Experimental data on ^{234}U(n, f), have been used in this work to study the influence of different neutron-multiplicity shapes. Based on the double-energy technique one cannot validate the one or the other method, because no prompt neutrons are detected in coincidence with the fission-fragment kinetic energies. However one may investigate the impact of the $\bar{\nu}(A)$ choice on the fission observables. Two methods were used in the analysis of the experimental data. In one case a higher $\bar{\nu}(A)$ was assumed for all fragment masses and in the other case a higher $\bar{\nu}(A)$ was only assumed for the heavy fragments. By comparing the two methods, the choice of $\bar{\nu}(A)$ was found to be important in the analysis of fission-fragments with relatively strong implications on the mass- and energy distributions. The results stress the need to determine $\bar{\nu}(A)$ by measuring fission fragments in coincidence with prompt-fission neutrons.

Selection and peer-review under responsibility of Joint Research Centre - Institute for Reference Materials and Measurements

Keywords: Neutron emission ; Sawtooth shape ; Fission fragment ; 2-E technique ; ^{234}U(n,f)

1. Background

The energy release in nuclear fission is given to the fission fragments (FF) either as kinetic- or excitation energy. The total excitation energy (TXE) in the fragments is shared between intrinsic excitation (single-particle like), deformation excitation as well as collective excitation (e.g. rotation). The fully accelerated fragments de-excite by emitting prompt neutrons followed by prompt-gamma rays and much later by beta-decay. The neutron multiplicity (ν), depends on the fragment deformation and shows the characteristic saw-tooth shape as a function of fragment mass as seen in Fig. 1(a). The data for ^{233,235}U(n, f) are taken from Ref. (Wahl, 1988). Due to the closed shells around $A = 132$ neutron evaporation is suppressed and results in a strong dip in $\bar{\nu}(A)$. Beside the mass dependency ν is also dependent on the TKE and the excitation energy in the compound nucleus. The total average neutron emission enhances with increasing incident-neutron energy. This, for example, can be seen in Fig. 1(b), where $\bar{\nu}_{\rm tot}(E_{\rm n})$, measured by (Mather

* Corresponding author. Tel.: +46-18-4715966.
Email addresses: Ali.Al-Adili@physics.uu.se (A. Al-Adili), Franz-Josef.HAMBSCH@ec.europa.eu (F.-J. Hambsch)

Selection and peer-review under responsibility of Joint Research Centre - Institute for Reference Materials and Measurements
doi:10.1016/j.phpro.2013.06.019

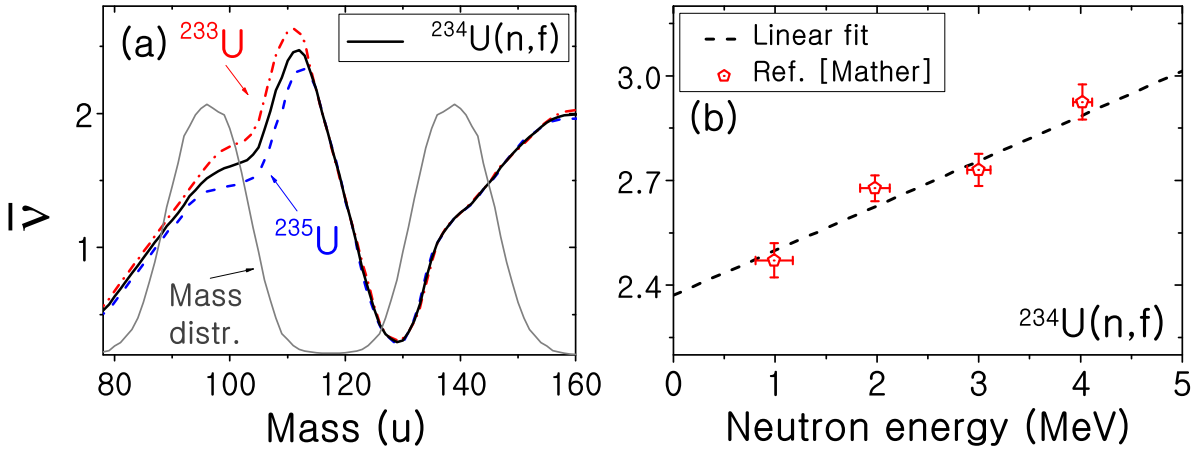

Figure 1. (a): The neutron multiplicity distributions from $^{233,235}\mathrm{U}\,(n,f)$ from Ref. (Wahl, 1988). $\nu_{234}\,(A)$ is determined as the average of the two neighbouring isotopes. The mass distribution for $^{234}\mathrm{U}\,(n,f)$ is shown as a guide-line. (b): The neutron emission increases as a function of excitation energy. The data are from Ref. (Mather et al., 1965).

et al., 1965) for $^{234}\mathrm{U}\,(n,f)$, is shown. The question is whether this increased neutron emission is mass-dependent or on average equal for the light and heavy fragments. A few early experiments have reported higher $\bar{\nu}\,(A)$ exclusively from the heavy fragments, leaving $\bar{\nu}_{\mathrm{light}}\,(A)$ practically unchanged (Naqvi et al., 1986; Müller et al., 1984; Bishop et al., 1970). Despite these experimental findings, many contemporary works still assume an average increase of $\bar{\nu}\,(A)$ as a function of excitation energy. For instance for $^{234,235,238}\mathrm{U}\,(n,f)$ (Al-Adili, 2013; Straede et al., 1987; Vivés et al., 2000) and $^{237}\mathrm{Np}\,(n,f)$ (Hambsch et al., 2000). Also in a few theoretical calculations $\bar{\nu}$ is increased for all masses, e.g. in Refs. (Vogt et al., 2012; Lestone et al., 2011; Yong-Jing and Ting-Jin, 2011). Recently, the shares of excitation energies have been treated theoretically by (Schmidt and Jurado, 2011; 2010). In the "energy-sorting" mechanism the observed increase of $\bar{\nu}\,(A)$ is attributed to the different fragment temperatures. In the pre-scission stage when the fragments are still connected through the neck, excitation energy may flow between the two fragments. Based on the constant-temperature behaviour described in Ref. (Egidy and Bucurescu, 2005), the fragment temperature is proportional to $A^{-2/3}$. Due to this, the heavy fragment is colder than the light one and the additional excitation energy will thus be transferred to the heavy fragment. The experimental observation supporting this energy transfer is the observed higher $\bar{\nu}_{\mathrm{heavy}}\,(A)$ and the unchanged $\bar{\nu}_{\mathrm{light}}\,(A)$, as a function of incident-neutron energy. The experimental data used in this study are based on a measurement of the kinetic energies of both fragments. The prompt-neutron multiplicity was not measured and needs to be parametrized in order to determine the final FF mass distributions. Therefore, these experimental data cannot bring a verification of the energy-sorting mechanism. However they can be used to investigate the possible changes in FF properties brought by assuming either of the correction methods, viz. an average increase versus a heavy-fragment increase of $\bar{\nu}\,(A)$.

2. Data Analysis

The study was performed on existing data from $^{234}\mathrm{U}\,(n,f)$ at 4 and 5 MeV incident-neutron energies. The data where measured at the 7 MV Van de Graaff accelerator of the IRMM in Geel, Belgium. Details on the setup and analysis can be found in Refs. (Al-Adili, 2013; Al-Adili et al., 2012a). The fragments were detected in a Twin Frisch-grid ionization chamber. The chamber has an anode and a Frisch-grid on each side providing information on the FF energy and emission angle, respectively. The angle was determined by using the grid method described in Ref. (Al-Adili et al., 2012b). The two fragments are emitted back-to-back which allows for using the double-energy (2E) technique. Conservation of momentum and mass requires that the ratio of the energies determine the masses:

$$m_1 = m_{\mathrm{cn}} E_2^{\mathrm{cm}} \left(E_1^{\mathrm{cm}} + E_2^{\mathrm{cm}}\right)^{-1} \quad \text{and} \quad m_2 = m_{\mathrm{cn}} E_1^{\mathrm{cm}} \left(E_1^{\mathrm{cm}} + E_2^{\mathrm{cm}}\right)^{-1} \quad , \tag{1}$$

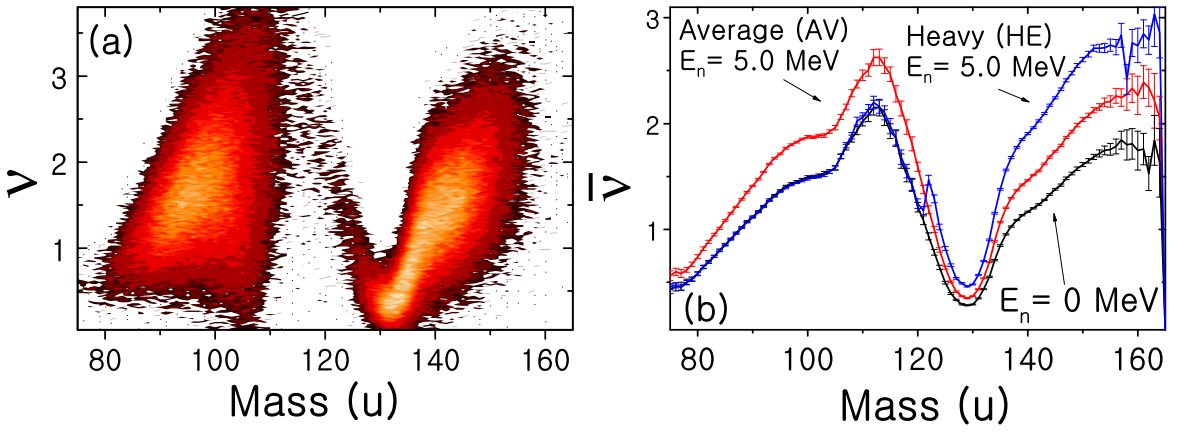

Figure 2. (a) The neutron emission as a function of mass and TKE. Data from Ref. (Al-Adili, 2013). (b) The two different correction methods for the higher neutron emission as a function of excitation energy.

where the compound nucleus mass m_{cn} is 235 u. The energies in the CM system are obtained by:

$$E_i^{\mathrm{cm}} = E_i^{\mathrm{lab}} \pm 2m_{\mathrm{cn}}^{-1}\sqrt{m_i m_{\mathrm{n}} E_i^{\mathrm{lab}} E_{\mathrm{n}}^{\mathrm{lab}}}\cos\left(\theta_i^{\mathrm{lab}}\right) + m_{\mathrm{cn}}^{-2} m_{\mathrm{n}} m_i E_{\mathrm{n}}^{\mathrm{lab}} \quad . \tag{2}$$

The (±) signs are due to the incoming neutron momentum. For one chamber side, all fragments get added momentum from the impinging neutron whereas on the other side they get a lower momentum. In order to obtain the energies in the laboratory system one has to assume the neutron emission on an event-by-event basis:

$$E_{\mathrm{pre}}^{\mathrm{lab}} \approx E_{\mathrm{post}}^{\mathrm{lab}} \frac{m_{\mathrm{pre}}}{m_{\mathrm{pre}} - \nu} \quad . \tag{3}$$

The recoil from the neutron emission is small and is neglected in Eq. (3). However it is crucial to account for the mass difference introduced by the different neutron emission. ν has to be parametrized as a function of mass, TKE and excitation energy. E_{post} for both FF are measured in the experiment and are used after applying various corrections for e.g. energy-losses and pulse-height defect. The neutron emission as a function of mass is seen in Fig. 1(a). $\bar{\nu}_{234}(A)$ was determined as the average of the neighbouring isotopes $\bar{\nu}_{233}(A)$ and $\bar{\nu}_{235}(A)$. Furthermore, the TKE dependence was obtained from the following expression:

$$\nu_{234}(A, \mathrm{TKE}) = \bar{\nu}_{234}(A) + \frac{\bar{\nu}_{234}(A)}{\bar{\nu}_{234}(A) + \bar{\nu}_{234}(A_{\mathrm{CN}} - A)} \times \frac{\langle \mathrm{TKE}(A) \rangle - \mathrm{TKE}}{E_{\mathrm{sep}}} \quad , \tag{4}$$

with a neutron separation energy of $E_{\mathrm{sep}} = 8.6$ MeV. The resulting experimental neutron emission shape is plotted in Fig. 2(a). The average total neutron emission has to reflect the values from the linear fit of Fig. 1(b). Therefore the distribution observed in Fig. 2(a) is increased by multiplying with a factor (α) to match $\bar{\nu}_{\mathrm{tot}}$ after weighting with the mass distribution. This increment is done in two different manners:

- ⋆ Average increase (AV): Implies that the whole $\bar{\nu}(A)$ distribution is increased for all fragment masses to match $\bar{\nu}_{\mathrm{tot}}$. This is seen in Fig. 2(b) as the highest $\bar{\nu}(A)$ distribution for $A < 120$.

- ⋆ Heavy increase (HE): Implies that the distribution for $A \geq 120$ is increased to match the value of $\bar{\nu}_{\mathrm{tot}}$. For $A <$ 120 the distribution is unchanged. This is seen in Fig. 2(b) as the highest $\bar{\nu}(A)$ distribution for $A > 120$.

In total, the average difference in $\bar{\nu}(A)$ between the two methods is about 26 % per fragment. The final pre-neutron emission mass distribution is calculated iteratively based on Eqs. (1, 2, 3). For each iteration the difference between

the newly determined mass and the previous mass is controlled. When the difference becomes smaller than 1/16 u the iterative process is stopped. The calculations fail to give integer values due to experimental resolution and the few approximations made in the analysis (mainly on the emitted neutrons). Once the masses have been determined they are rounded to the nearest integer mass which also leaves an integer ν.

3. Results

A detailed discussion of all the results was presented in Ref. (Al-Adili et al., 2012c). The HE method, in contrast to the AV method, increases the neutron emission from the heavy mass and reduces $\bar{\nu}(A)$ from the light fragments. Therefore it naturally leads to the mean positions of the heavy and light fragments being closer to each other. The observed effects were growing with the incident-neutron energy. Moreover, the changes were twice as large in the post-neutron emission distributions compared to the pre-neutron emission ones. The average total kinetic energy distributions ($\overline{\mathrm{TKE}}$) showed about 0.2 MeV difference, for E_n = 5.0 MeV. These changes where mass-dependent as shown in Fig. 3(a). The largest deviations are encountered around the mass $A \approx 132$ u. The single fragment kinetic energies, $\overline{E}_\mathrm{kin}$, show changes up to 0.75 MeV in the post-neutron emission as seen in Fig. 3(b). The lower energies are found for the heavy fragments whereas on the light fragments, $\overline{E}_\mathrm{kin}$ is slightly higher for the HE method. These differences between the light and heavy fragments are due to the special shape of the $\overline{E}_\mathrm{kin}$ as a function of mass, which stays nearly constant for the light fragments and changes strongly for the heavy fragments. The mass distributions were also affected. The average heavy-fragment mass shifted by 0.68 u for the post-neutron emission masses of E_n = 5.0 MeV. The effect was twice of that in the pre-neutron distributions. In terms of the absolute yield difference as a function of mass, the largest changes were seen around A = 90, 102, 132 and 145. Absolute yield changes reach almost up to 1.0% difference, which is a large effect considering the maximum probable fission yield reaches 6-7%. In relative terms, the changes in mass are shown in Fig. 3(c), where the ratio of mass yield analysed using the HE- as well as with the AV-method is plotted. Relatively, the difference can reach up to 10-30%, for different mass regions. In the pre-neutron emission mass distributions, the σ_TKE and σ_A were less affected and were within experimental uncertainty. However for the post-neutron masses the differences were more severe.

In general, the observed effects were significant. Since many measurements were analysed assuming using the AV method, these data are also affected if HE proves to be the valid approach. The differences in average distribution values were estimated and are presented in Eqs. (5, 6, 7). The changes in $\overline{\mathrm{TKE}}$ and $\langle A^\mathrm{pre}\rangle$ were fitted linearly as seen in Fig. 3(d). The changes fitted were $\Delta\overline{\mathrm{TKE}} = \overline{\mathrm{TKE}}_\mathrm{AV} - \overline{\mathrm{TKE}}_\mathrm{HE}$ and $\Delta\langle A_\mathrm{H}\rangle = \langle A_\mathrm{H}\rangle_\mathrm{AV} - \langle A_\mathrm{H}\rangle_\mathrm{HE}$. These formulae provide a good approximation for the expected shift in $\langle A^\mathrm{pre}\rangle$ and $\overline{\mathrm{TKE}}$ since the distributions are mostly shifted. In the case of $\langle A^\mathrm{post}\rangle$, a mere shift is probably not sufficient to account for the changes.

$$\overline{\mathrm{TKE}}_\mathrm{HE} \approx \overline{\mathrm{TKE}}_\mathrm{AV} - 0.038 \times E_\mathrm{n} \ \ (\mathrm{MeV}) \tag{5}$$

$$\langle A_\mathrm{H}^\mathrm{pre}\rangle_\mathrm{HE} \approx \langle A_\mathrm{H}^\mathrm{pre}\rangle_\mathrm{AV} - 0.065 \times E_\mathrm{n} \ \ (\mathrm{u}) \tag{6}$$

$$\langle A_\mathrm{H}^\mathrm{post}\rangle_\mathrm{HE} \approx \langle A_\mathrm{H}^\mathrm{post}\rangle_\mathrm{AV} - 0.135 \times E_\mathrm{n} \ \ (\mathrm{u}) \tag{7}$$

4. Conclusions

In this work we investigated the consequence of two different assumptions on the neutron emission from fission fragments. The assumption is crucial in the analysis based on the 2E-technique since no neutrons are measured in coincidence with the fragments. Both methods fully account for the increase in $\bar{\nu}_\mathrm{tot}$. In one case however, the neutron multiplicity was increased independent of the fragment mass. In the second case, only the heavy fragments were assumed to emit the extra neutrons. A significant difference in FF observables was recorded when applying either of the two neutron-correction methods denoted as AV and HE. These results affect all FF measurements done without precise knowledge on $\bar{\nu}(A)$. Due to this, many fission yield measurements (mainly post-neutron emission masses) in the data libraries may show discrepancies up to 10-30 %. Energy distributions were also affected. Therefore, it is crucial to determine $\bar{\nu}(A)$, with the dual support from theoretical models and from experimental investigation. The few measurements on the exclusive heavy-fragment emission of the extra neutrons are not enough since the average approach is still assumed in many works. Therefore, this study urges for further FF measurements as a function of E_n and in coincidence with $\bar{\nu}(A)$ measurement.

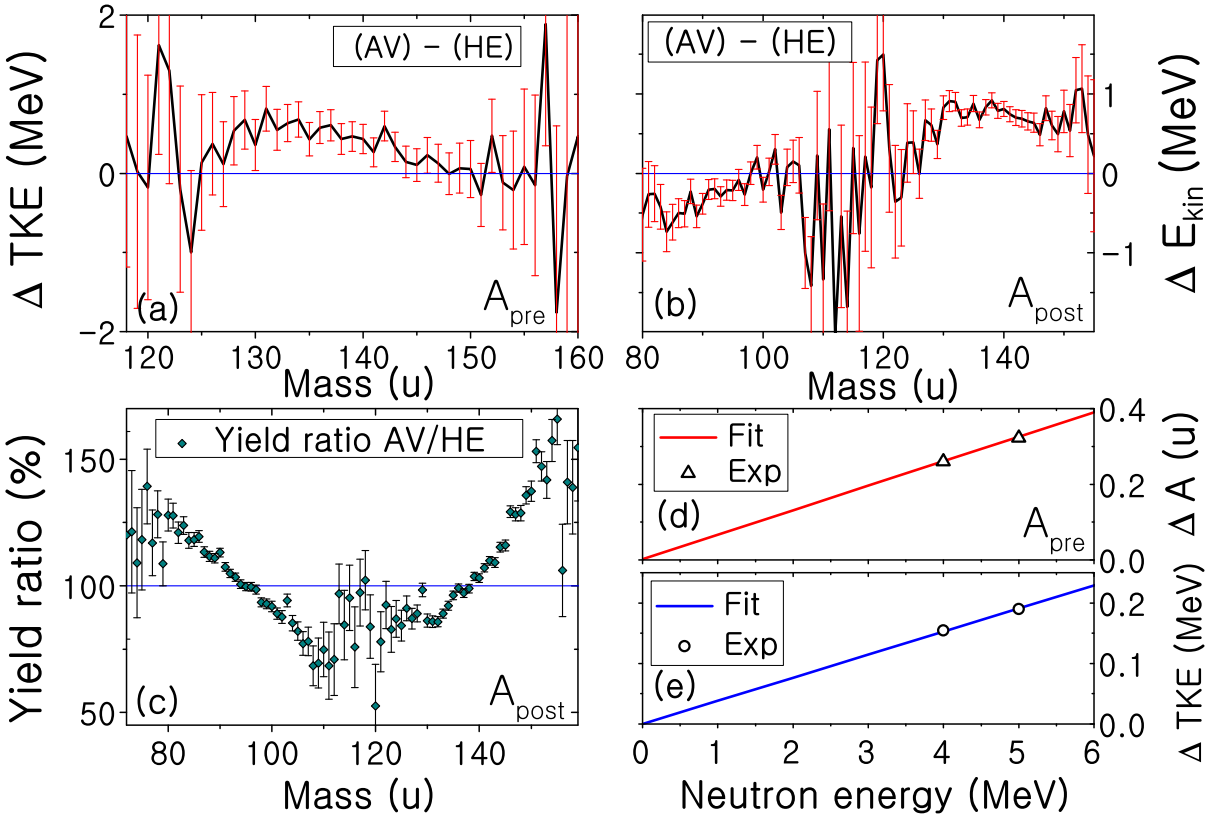

Figure 3. (a) The changes in $\overline{\mathrm{TKE}}$ are mass-dependent and reach more than 0.5 MeV. (b) The changes in the single fragment energy, $\overline{E}_{\mathrm{kin}}$ show up to 0.75 MeV differences. (c) The relative differences in $\langle A^{\mathrm{post}} \rangle$ reach between 10 and 30 %. (d) The change in $\langle A^{\mathrm{pre}} \rangle$ as a function of E_{n}. (e) The change in $\overline{\mathrm{TKE}}$ as a function of E_{n}.

Acknowledgements

A. A. is indebted to the Joint Research Centre (IRMM) of the European Commission, for granting him a Ph.D. fellowship.

References

Al-Adili A., "Measurements of the ^{234}U(n,f) Reaction...", 2013. Ph.D. thesis, Uppsala University, Sweden.
Al-Adili A., Hambsch F.-J., Oberstedt S., Pomp S., 2012. Phys. Procedia 31, 158.
Al-Adili A., Hambsch F.-J., Bencardino R., Pomp S., Oberstedt S., Zeynalov Sh., 2012. Nucl. Meth. Instr. A671, 103.
Al-Adili A., Hambsch F.-J., Pomp S., Oberstedt S., 2012. Phys. Rev. C86, 054601.
Bishop C. J., Vandenbosch R., Aley R., Shaw R. W., Halpern I., 1970. Nucl. Phys. A150, 129.
Egidy T., Bucurescu D., 2005. Phys. Rev. C72, 044311.
Hambsch F.-J., Vivés F., Siegler P., Oberstedt S., 2000. Nucl. Phys. A679, 3.
Lestone J. P., 2011. Nucl. Data Sheets 112, 3120.
Manailescu C., Tudora A., Hambsch F.-J., Morariu C., Oberstedt S., 2011. Nucl. Phys. A867, 12.
Mather D. S., Fieldhouse P., Moat A., 1965. Nucl. Phys. 66, 149.
Müller R., Naqvi A. A., Käppeler F., Dickmann F., 1984. Phys. Rev. C29, 885.
Naqvi A. A., Käppeler F., Dickmann F., Müller R., 1986. Phys. Rev. C34, 218.
Schmidt K.-H., Jurado B., 2011. Phys. Rev. C83, 061601.
Schmidt K.-H., Jurado B., 2010. Phys. Rev. Lett. 104, 212501.

Straede C., Budtz-Jørgensen C., Knitter H.-H., 1987. Nucl. Phys. A462, 85.
Vivés F., Hambsch F.-J., Bax H., Oberstedt S., 2000. Nucl. Phys. A662, 63.
Vogt R., Randrup J., Brown D. A., Descalle M. A., Ormand W. E., 2012. Phys. Rev. C85, 024608.
Wahl A. C., 1988. At. Data and Nucl. Data Tab. 39, 1.
Yong-Jing Chen, Ting-Jin Liu, 2011. CPC 35, 344.